Virus Evolution, 2021, 7(1): veab043

doi: 10.1093/ve/veab043
Research Article

Two distant helicases in one mycovirus: evidence of horizontal gene transfer between mycoviruses, coronaviruses and other nidoviruses

Assane Hamidou Abdoulaye,[1,2,†] Du Hai,[1,2,†] Qing Tang,[3] Daohong Jiang,[1,2] Yanping Fu,[2] Jiasen Cheng,[1,2] Yang Lin,[2] Bo Li,[1,2] Ioly Kotta-Loizou,[4] and Jiatao Xie[1,2,*,‡]

[1]State Key Laboratory of Agricultural Microbiology, Huazhong Agricultural University, Wuhan, Hubei Province 430070, People's Republic of China, [2]Hubei Key Laboratory of Plant Pathology, College of Plant Science and Technology, Huazhong Agricultural University, Wuhan, Hubei Province 430070, People's Republic of China, [3]Xiangyang Academy of Agricultural Sciences, Xiangyang, Hubei Province, 441057, People's Republic of China and [4]Department of Life Sciences, Imperial College London, London SW7 2AZ, UK

*Corresponding author: E-mail: jiataoxie@mail.hzau.edu.cn

†These authors contributed equally to this work.

‡https://orcid.org/0000-0003-1961-0338

Abstract

Nidovirales, which accommodates viruses with the largest RNA genomes, includes the notorious coronaviruses; however, the evolutionary route for nidoviruses is not well understood. We have characterized a positive-sense (+) single-stranded (ss) RNA mycovirus, Rhizoctonia solani hypovirus 2 (RsHV2), from the phytopathogenic fungus *Rhizoctonia solani*. RsHV2 has the largest RNA genome size of 22,219 nucleotides, excluding the poly(A) tail, in all known mycoviruses, and contains two open reading frames (ORF1 and ORF2). ORF1 encodes a protein of 2,009 amino acid (aa) that includes a conserved helicase domain belonging to helicase superfamily I (SFI). In contrast, ORF2 encodes a polyprotein of 4459 aa containing the hallmark genes of hypoviruses. The latter includes a helicase belonging to SFII. Following phylogenetic analysis, the ORF1-encoded helicase (Hel1) unexpectedly clustered in an independent evolutionary branch together with nidovirus helicases, including coronaviruses, and bacteria helicases. Thus, Hel1 presence indicates the occurrence of horizontal gene transfer between viruses and bacteria. These findings also suggest that RsHV2 is most likely a recombinant arising between hypoviruses and nidoviruses.

Key words: mycovirus; hypovirus; nidoviruses; coronaviruses; helicase; HGT; recombination.

1. Introduction

Horizontal gene transfer (HGT) is the genetic material transmission between distantly related organisms and leads to ecologically significant features (Gogarten and Townsend 2005; Keeling and Palmer 2008). HGT is prevalent in archaea, bacteria, and viruses; nevertheless, its relevance and scale in eukaryotes

remain contentious (Alexander et al. 2016). HGT often relies on biological interaction via endosymbiotic mechanisms. HGT impact varies depending on the lineage, and most affected lineages are the least studied at the genomic level, such as the protists (Keeling and Palmer 2008). Several investigations have described prokaryotic gene transmission into the fungal genome and gene transmission between fungi (Marcet-Houben and Gabaldón 2010; Wisecaver et al. 2014; Wisecaver and Rokas 2015). Notably, HGT frequency is generally higher in prokaryote genomes as compared to eukaryotes (Andersson 2009). However, gene integration into an organism is usually constrained by selective barriers. HGT's prime example between bacteria, where surface exclusion, restriction sites, and plasmid replication and establishment in a heterologous host, are all likely barriers to HGT in prokaryotes (Thomas and Nielsen 2005). In addition, the cell structure and conflicting compatibility between donor and recipient are potential barriers to HGT in eukaryotes (Keeling and Palmer 2008; Richards et al. 2011). HGT also occurs from cellular organisms to viruses but rarely occurs from viruses to cellular organisms, except retroviruses and some DNA viruses (Liu et al. 2010; Liu et al. 2011). For example, endogenous lentiviruses are present in the rabbit genome (Katzourakis et al. 2007), and geminiviral DNA is inserted in the *Nicotiana tabacum* genome (Bejarano et al. 1996).

RNA viruses have evolved substantial variability to adapt in living organisms, particularly due to environmental transition through evolution (Aaziz and Tepfer 1999). Viral RNA recombination (VRR) involves the exchange of genetic material between associated viral RNAs and results in a recombinant viral genome (Nagy and Simon 1997). VRR occurs randomly and rarely, and the recombination mechanism is still a matter of debate. For instance, three types of VRR are known so far: (1) homologous recombination, (2) aberrant homologous recombination, and (3) non-homologous recombination (Lai 1992). The relative recombination relevance varies at the genomic level and is known as the main driver of viral evolution (Bentley and Evans 2018). Furthermore, homologous recombination helps to maintain genome integrity (Crickard et al. 2020).

Mycoviruses are prevalent in all major fungi groups (Ghabrial et al. 2015; Son et al. 2015). The majority of mycoviruses belong to class III (double-stranded [ds]RNA) of the Baltimore virus classification, while thirty per cent belong to class IV (positive-sense single-stranded [+ss]RNA) (Baltimore 1971; Son et al. 2015). The knowledge about the diversity of known mycoviruses has dramatically increased over the past five years due to the development of new research approaches (Nerva et al. 2016; Kotta-Loizou and Coutts 2017; Sahin and Akata 2018). Nevertheless, countless mycoviruses remain undiscovered (Son et al. 2015). According to the International Committee for the Taxonomy of Viruses (ICTV), mycoviruses are currently classified into twenty-five officially recognized families and a floating non-classified genus. The discovery of hypoviruses, capsidless viruses with a (+)ssRNA genome, revolutionized virocontrol and led to the term 'hypovirulence', a phenomenon that could be exploited in the context of sustainable biological control of fungal diseases. *Hypovirus* is the sole genus of the family *Hypoviridae* and contains four officially recognized species and were recently assigned to the realm *Riboviria* by the ICTV (Suzuki et al. 2018). Unclassified hypoviruses are frequently encountered and were characterized from multiple fungal species (Suzuki et al. 2018).

The viruses with the largest RNA genomes belong to the order *Nidovirales*. According to the ICTV, *Nidovirales* accommodates eight suborders and fourteen families, such as *Coronaviridae*, which have (+)ssRNA genomes ranging in size from 26 to 32 kb within crown-like virions (Su et al. 2016). Animals and fungi interactions involve mutualism, commensalism, and parasitism and are frequently infected with viruses (Ghabrial et al. 2015; Loeffelholz and Fenwick 2021). Evolutionary analyses of mycoviruses families such as *Genomoviridae* indicate a close relationship with animal viruses (Lamberto et al. 2014). However, fungi share very few viral signatures with animal viruses (Roossinck 2019).

Rhizoctonia solani (Teleomorph: *Thanatephorus cucumeris*), a soil-borne fungus, is a phytopathogenic basidiomycete known to cause many important diseases in various crops, including rice, wheat, and maize (Xia et al. 2017). Several mycoviruses infecting *R. solani* have been detected *via* either conventional dsRNA extraction or high-throughput sequencing approaches (Wang et al. 2009). The latter revealed that *R. solani* harbors a rich and complex virome (Picarelli et al. 2019). Therefore, *R. solani* mycoviruses investigations could enhance our understanding of mycoviral diversity and ecology. We identified and characterized a chimeric RNA mycovirus, Rhizoctonia solani hypovirus 2 (RsHV2), with two ORFs. RsHV2 has the largest genome among the known mycoviruses. The RsHV2 polyprotein shared high identity with *Hypoviridae* members. The helicase encoded by RsHV2 ORF1 is related to those found in bacteria and members of *Nidovirales*, suggesting that HGT of helicases occurred between viruses and bacteria. Furthermore, examination of the RsHV2 genome revealed a potential recombination event between hypoviruses and *Nidovirales* members.

2. Materials and methods

2.1 Fungal strain isolation, culture conditions, and identification

R. solani strains XN84 and ES63 were isolated from diseased rice plant tissues, respectively, collected in Xianning and Enshi County, Hubei Province, China. Strains XN84VF and ES63 are RsHV2-free strains. XN84VF is a derivative of XN84 resulting from single protoplast isolation. An internal transcribed spacer region was amplified through polymerase chain reaction (PCR) amplification and sequenced to confirm the provenance of both *R. solani* isolates (Fiers et al. 2011). Fungal strains were cultured on potato dextrose agar (PDA) at an optimum temperature of 28 °C with a photoperiod of 16 h/8 h (day/night).

2.2 Protoplast and hyphal tip isolation

Protoplasts were prepared from strain XN84 following the procedure described previously (Feng et al. 2012), with slight modifications. First, fresh mycelia were collected from sterilized cellophane membranes placed onto PDA and used to inoculate flasks containing 100 ml PD broth. After 12-h growth with shaking at 180 rpm, mycelia were ground with a mortar and pestle, suspended into a fresh liquid medium, harvested by filtering through layers of gauze, and washed with osmoticum (0.7 M $MgSO_4$). Mycelial homogenates were resuspended in a filter-sterilized enzyme mixture of cellulase (Sigma-Aldrich, 8 mg/ml), driselase (Sigma-Aldrich, 10 mg/ml), and lysing enzymes (Sigma-Aldrich, 10 mg/ml) and incubated under shaking at 28 °C for 3 h. The protoplasts were monitored with a hemocytometer and microscope every 0.5 h until sufficient numbers were released. The enzyme mixture was then removed with a 120-μm pore size nylon mesh. The protoplasts suspension was centrifuged at 3,000 × *g* for 10 min, washed twice with osmoticum,

and resuspended in an appropriate STC volume (1 M sorbitol, 50 mM Tris-HCl pH 8, 50 mM $CaCl_2$). The resultant protoplasts were spread onto the regeneration medium (RM) surface to record their regeneration rate. Single-protoplast isolates were obtained and cultured on PDA. Mycelial plugs selected from the colony margin of regenerated isolates were grown on PDA for one day. Single hyphal tips were removed using a sterilized needle and inoculated on fresh PDA. This procedure was conducted at least seven times. The colony morphology of all regenerated isolates was observed, and total RNA was extracted to detect mycovirus.

2.3 Horizontal transmission assay

To investigate mycovirus horizontal transmission through hyphal anastomosis, mycelial agar plugs from the donor and recipient strains XN84 and ES63, respectively, were dual-cultured on PDA (Zhang et al. 2009). At a time point between 24 and 72 h, mycelial agar plugs were taken from the side of the recipient strain ES63 distant from the contact line between the two colonies and cultured on fresh PDA. This procedure was repeated at least three times. The virus-reinfected isolates were further subjected to dsRNA isolation and mycovirus detection via reverse transcription PCR (RT-PCR) amplification.

2.4 Virulence assay

Virulence assays of both *R. solani* strains XN84 and XN84VF were conducted on rice leaves (*Oryza sativa*). Here, isogenic lines of XN84 and XN84VF were initially cultured on PDA, and mycelial plugs of each were inoculated on newly grown rice leaves and incubated in a growth chamber at 28 °C. Lesion sizes were measured up to 5 days post-inoculation (dpi). All inoculations were repeated at least three times.

2.5 Nucleic acid isolation, purification and northern hybridization

R. solani strains XN84 and XN84VF were cultured on sterilized cellophane membranes placed on Petri dishes containing PDA. The fresh mycelia (2 dpi) were harvested and ground to a fine powder with liquid nitrogen using a sterilized mortar and pestle. Isolation and purification of dsRNA were performed using CF-11 cellulose (Sigma-Aldrich, USA) following a previously described procedure (Xie et al. 2006) with minor modifications. The extracted dsRNA samples were suspended in sterile double-distilled water (ddH_2O) or diethyl pyrocarbonate-treated water (DEPC-H_2O) and then digested with S1 nuclease and DNase I (Takara, China). The dsRNA segment purification was performed using a gel extraction kit (Axygen Scientific Inc., China), and all samples were stored at −80 °C.

Total RNA isolation was conducted with the TRIzol Reagent Extraction Kit (Takara, China) according to the manufacturer's instructions with slight modifications. Here 1 ml of TRIzol reagent was added to ground mycelial powder and the mixture maintained on ice until stratification. The supernatant was precipitated at −20 °C with isopropyl alcohol or ethanol. The nucleic acid pellet was collected, washed with seventy per cent ($^{v}/_{v}$) ethanol, and dissolved in ddH_2O or DEPC-H_2O. Total RNA was used in RT-PCR amplification or subjected to RNA-seq analysis.

Northern hybridization was conducted to investigate mycoviruses infecting strain XN84. Briefly, the RNA molecules were size fractionated by one per cent ($^{w}/_{v}$) agarose/TAE (40 mM Tris/acetic acid, 1 mM EDTA, pH 7.6) gel electrophoresis for 4 h at 4 °C. The gel was then soaked in 0.1 M NaOH followed by 0.1 M Tris/HCl (pH 8.0) for 20 min on each solution. Then, the RNA was transferred onto a membrane (Amersham Hybond-N+ nylon, GE Healthcare) in 10× SSC buffer by capillary action and covalently bound (Jiang and Ghabrial 2004). A probe was produced by RT-PCR amplification of the complete RsHV2 genome and radioactively labeled for subsequent detection purposes. Hybridization was detected by autoradiography using a BIORAD Fluorescent Image Analyzer (Bio-Rad, China).

2.6 Rapid amplification of cDNA ends

The 5′ and 3′ terminal sequences of the putative viruses were determined as previously described (Potgieter et al. 2009) with slight modifications. The dsRNA was first subjected to gel purification following the manufacturer's recommendation. The terminal sequences of the purified dsRNA segments were ligated to the PC3-T7 loop (5'-p-GGA TCC CGG GAA TTC GGT AAT ACG ACT CAC TAT ATT TTT ATA GTG AGT CGT ATT A-OH-3′) using T4 RNA ligase buffer (Takara, Dalian, China), PEG 6000, Bis (trimethylsilyl) acetamide, recombinant RNase inhibitor and T4 RNA ligase (40 U/μl). The mixture was incubated at 4 °C for 18 h, following denaturation of the RNA with DMSO. The purified ligated dsRNA was used as a template for cDNA synthesis. The cDNA was then amplified with a specific primer (3′-TGA CCC TCG TAT CCA GCA GA-5′ and 5′-TGA CGA TAG CAG GGA GGG AA-3′ for the 3′ and 5′ ends, respectively) as the forward primer and a sequence complementary to the PC3-T7 loop, PC2 (5′-p-CCG AAT TCC CGG GAT CC-3′), as the reverse primer. The amplicons obtained underwent gel purification and were cloned into the pMD18-T vector (Takara, China). At least four independent clones were then sequenced.

2.7 NGS analysis for mycovirus identification

The *R. solani* strain XN84 metatranscriptome library was constructed using the TruSeq™ RNA Sample Prep Kit (Illumina, USA) and sequenced by the Shanghai Biotechnology Corporation Company using Illumina HiSeq 2000/2500. Prior to further analysis, the raw reads were filtered to remove: (1) whole reads of low-quality overall; (2) low-quality bases at the 3′ end of reads; (3) adapter sequences; (4) ambiguous N bases; (5) sequencing fragments less than 20 nt in length; and (6) host rRNA and mRNA sequences. *De novo* assembly of the remaining, high-quality reads was performed using a contig scaffolding algorithm (CLC Genomics Workbench 6.0.4) (Bräutigam et al. 2011; Garg et al. 2011; Su et al. 2011). The first sequence, called the primary UniGenes, was obtained. The primary UniGenes were then spliced twice, with CAP3 EST software, to obtain the first and second contigs. The contigs obtained were subjected to data analysis with online tools (https://blast.ncbi.nlm.nih.gov/Blast.cgi).

2.8 Computational sequence analysis

Nucleotide sequence assembly and translation were executed with DNAMAN 7.0 and Geneious 5.6.5 (Kearse et al. 2011; Parrella et al. 2013). Different tools were used to determine and analyze the putative ORFs, including the online NCBI ORF Finder tool (http://www.ncbi.nlm.nih.gov/projects/gorf). Multiple sequence alignment was performed with MEGA X (Kumar et al. 2018) to determine conserved protein motifs. Putative transmembrane (TM) regions were determined with the online program TMHMM 2.0 (http://www.cbs.dtu.dk/services/TMHMM/) (Anders Krogh et al. 2001). Phyre2 was used to

predict the three-dimensional (3D) structure of protein sequences *via* homology modeling based on an alignment generated by the hidden Markov model (HMM) matching (Kelley et al. 2015). The predicted structures were visualized with PyMOL. The online tool T-Coffee (http://tcoffee.crg.cat/apps/tcoffee/index.html) was applied for sequence alignment. To determine the evolutionary relationships between the newly identified and previously recognized viruses, phylogenetic analysis was performed with MEGA by constructing maximum likelihood phylogenetic trees, using best-fit substitution models LG + G or WAG + G + I (selected by SMS: Smart Model Selection in PhyML), with 1,000 bootstrap replicates (Kumar et al. 2018). The RNA secondary structure of untranslated regions (UTRs) was predicted, and the initial energy was calculated using the online program Mfold (http://mfold.rna.albany.edu/?q=mfold/RNA-Folding-Form) (Zuker 2003). Oligonucleotide primers were designed using Primer-BLAST (https://www.ncbi.nlm.nih.gov/tools/primer-blast/). The reads distribution profile from metatranscriptomic data was displayed with the interactive tool Integrative Genomics Viewer (IGV) (Robinson et al. 2017).

3. Results

3.1 A novel virus with the largest genome among all known mycoviruses

R. solani strain XN84 showed abnormal phenotypic traits in terms of colony morphology and virulence as compared to other isolates (Fig. 1A and 1B) and was suspected to harbor one or multiple mycoviruses. High-throughput sequencing was conducted to investigate mycoviruses in strain XN84. A total of *ca.* 10 Gb data were generated after filtering out the low-quality reads. All reads that did not match the *R. solani* genome were assembled. Following this, a contig5677, 22,210-bp long, was generated. Homology searches of the contig5677 sequence against the NCBI virus amino acid (aa) sequence database (BLASTx) revealed that contig5677 contained a sequence that was partially related to *Hypoviridae* members and displayed similarity to Rhizoctonia solani hypovirus 1 (RsHV1; accession number: QDW92698.1, E-value = 0.0), Monilinia hypovirus A (MoHVA; accession number: QED42922.1, E-value = 0.0, a partial genome) and Sclerotinia sclerotiorum hypovirus 2 (SsHV2; accession number: QBA69886.1, E-value 3e-97). Thus, contig5677 was a partial genome sequence of a mycovirus related to hypoviruses. This newly discovered mycovirus was provisionally termed Rhizoctonia solani hypovirus 2 (RsHV2). RsHV2 has the largest genome among previously described mycoviruses. The transcriptomic reads distribution profile displayed more reads at the 3′ends than the 5′ends (Fig. 1E).

RT-PCR amplification was conducted with contig5677-specific primers to confirm that strain XN84 harbored RsHV2. As predicted, an amplicon of 1,803 bp was produced (Supplementary Fig. S1A) that was identical in sequence to the contig5677. Hypoviruses have (+)ssRNA genomes with a dsRNA intermediate replicative form, as previously reported (Suzuki et al. 2018). Thus, dsRNA was extracted from the fungal mycelia and subsequently treated with S1 nuclease and DNase I (Fig. 1C and Supplementary Fig. S2A). High-throughput sequencing analysis revealed that strain XN84 harbored three mycoviruses including two mitoviruses and RsHV2 (Supplementary Table S1), which were confirmed following RT-PCR amplification (Supplementary Fig. S1A). XN84 dsRNA gel-electrophoresis showed two segments corresponding to putative mitovirus genomes, and a larger segment (approximately 23 kb based on the DNA molecular weight marker) considered to be the dsRNA representative of the RsHV2 genome. To further confirm the existence and genome size of RsHV2, northern blotting was conducted, and the results of which are shown in Fig. 1C.

3.2 RsHV2 has two ORFs that encode two phylogenetically distant helicases

The full-length contig5677 (partial sequence of RsHV2) was amplified through serial RT-PCR amplification, using contig5677-specific primers, to confirm the accuracy of the assembled sequence (Supplementary Table S2A and Fig. S1B). The 5′ and 3′ terminal sequences of RsHV2 were determined to obtain the RsHV2 complete genomic sequence, resulting in an RsHV2 full-length cDNA (Fig. 1D). The RsHV2 genome contains 22,219 nt excluding the poly(A) tail and has a nucleotide composition of 26.0 per cent A, 22.5 per cent T, 27.5 per cent C, and 24 per cent G. The 5′ and 3′ UTRs were 826 nt and 1,161 nt in length, respectively. The terminal sequences (5′ and 3′ UTRs) can form potential stem-loop structures with energies of −57.10 and −20.99 kcal/mol, respectively (Supplementary Fig. S3A). These secondary structures protect messenger RNA (mRNA) structural stability, supply RNA binding protein recognition sites, and act as enzymatic reaction substrates (Svoboda and Cara 2006).

RsHV2 contains two predicted large ORFs, ORF1 (6027 nt) and ORF2 (13377 nt), on the positive strand. An intergenic region of 825 nt separates the two ORFs. ORF1 (827–6854 nt) encodes a putative protein of 2,009 aa in length with a molecular mass of 225 kDa. The conserved domain search revealed that the ORF1-encoded protein has only two conserved domains: (1) a viral RNA helicase (Hel1; 315-554 aa) and (2) a late cornified envelope-like proline-rich protein 1 (Lelp1; 1708-1778 aa) that usually found in mammals (Fig. 1D and Supplementary Fig. S3B). ORF2 (7,679–21,058 nt) encodes a putative polyprotein of 4,459 aa in length with a molecular mass of 504 kDa that contains three conserved domains: (1) a putative papain-like protease (Pro; 244-352 aa), (2) an RNA-dependent RNA polymerase (RdRp; 2,802–3,239 aa), and (3) a DEAD-like helicase (DEXDc; 3,671–3,984 aa), displaying similar structures to those found in hypoviruses such as SsHV2 (Krogh 2001). In addition, two TM domains were found in the ORF2-encoded polyprotein (Fig. 1D).

Interestingly, multiple sequence alignment and phylogenetic tree analysis indicated that the Hel1 is most closely related to the helicases belonging to the superfamily I (SFI). In contrast, the ORF2-encoded helicase (Hel2) is an SFII helicase. This result suggests that RsHV2 is a potential recombinant mycovirus. Therefore, it is assumed that an HGT might be involved in the acquisition of a helicase SFI gene by RsHV2.

3.3 RsHV2 is distantly related to hypoviruses

Multiple sequence alignment of the ORF2-encoded polyprotein and its three conserved domains were conducted to understand the phylogenetic relationship between RsHV2 and other previously characterized viruses. Pairwise sequence comparisons showed that the RsHV2 ORF2-encoded polyprotein shares 49.52 per cent, 24.43 per cent, and 27.85 per cent aa identity with, respectively, RsHV1 (68% coverage), Sclerotium rolfsii hypovirus 1 (SrHV1; accession number: AZA15168.1, 61% coverage), and SsHV2 (60% coverage). Furthermore, phylogenetic analysis based on hypovirus polyproteins suggested that all the selected hypoviruses could be classified into eight groups (I to VIII), and RsHV2 belongs to group IV most closely related to members of groups I and III (Fig. 2). Notably, six groups were previously

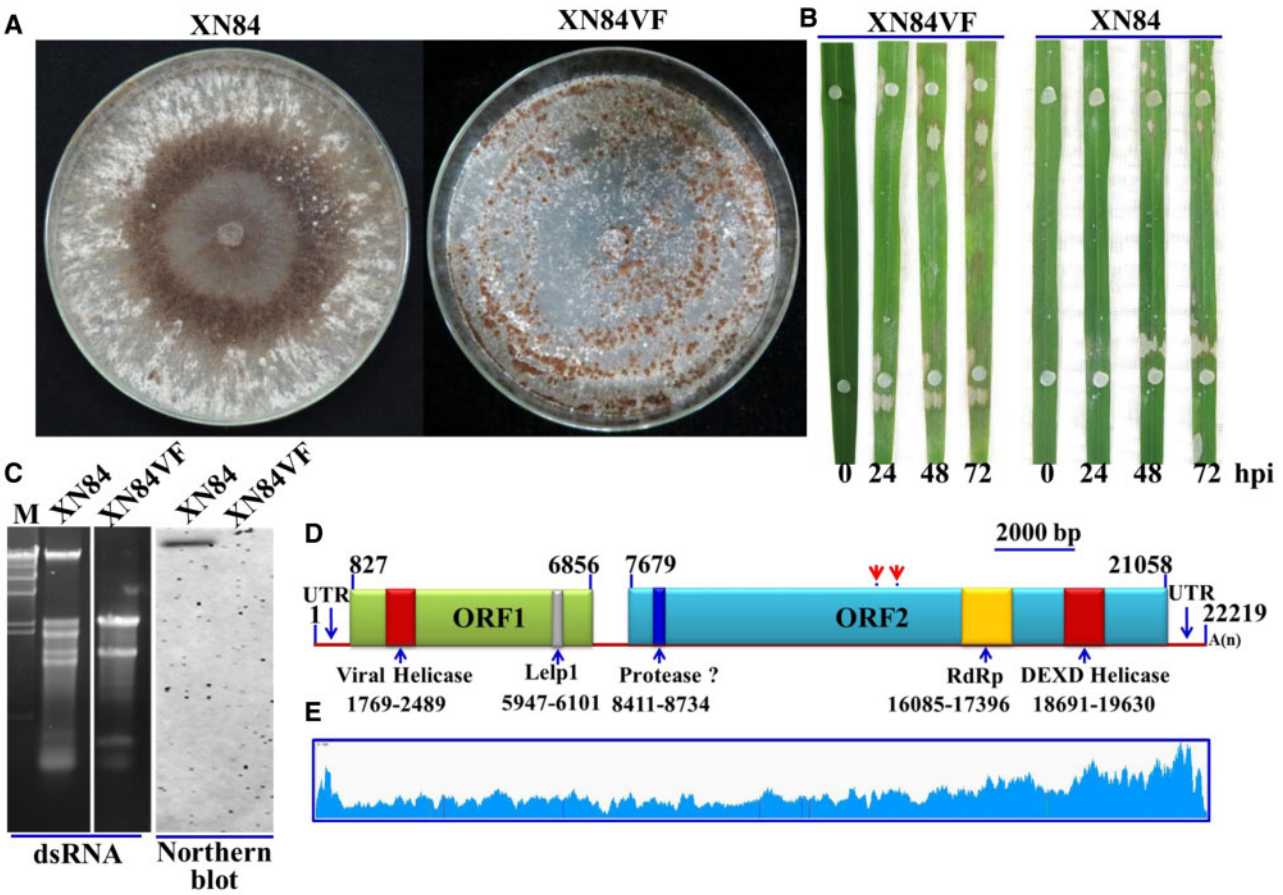

Figure 1. RsHV2 was discovered in *R. solani* strain XN84. (A) Colony morphology of the RsHV2-infected strain XN84 and the RsHV2-free strain XN84VF (25 °C, 5 dpi). (B) Pathogenicity test of XN84 and XN84VF on fresh rice leaves. Picture were taken 24 h post-inoculation (hpi), 48 hpi and 72 hpi. (C) Agarose gel electrophoresis of dsRNAs extracted from strain XN84 (left panel) and northern hybridization (right panel) of RsHV2. The M (Kbp) lane corresponds to DNA marker λ-Hind III expressed in kilobase pairs (kbp). (D) Schematic representation of the genomic organization of RsHV2. The two rectangles represent the two putative ORFs. ORF1 encodes a putative protein with two conserved motif domains: Viral_Helicase1 (pfam01443, E-value = 2e−07) and Late cornified envelope-like proline-rich protein 1 (Lelp1, pfam15042, E-value = 2.31e−03). ORF2 encodes a polyprotein that includes a DEAD-like helicase (DEXDc, smart00487) and an RNA-dependent RNA polymerase (RdRp) domain. In addition, ORF2 encoded a predicted papain-like protease (PRO) based on multiple sequence alignments. Two TM domains were predicted and marked by red arrows. (E) Mapping of sequencing reads on the RsHV2 genome.

proposed based on hypovirus polyproteins analysis (Wang et al. 2013; Khalifa and Pearson 2014; Li et al. 2015; Li et al. 2020).

The putative protease located at the N terminus of the ORF2-encoded polyprotein contains conserved cysteine and histidine residues necessary for autoproteolytic activity, and a glycine residue associated with the potential cleavage site (Yuan and Hillman 2001) (Supplementary Fig. S5A). The putative protease shares a considerably lower identity (12%–19%; Supplementary Table S2B) with hypovirus proteases (Supplementary Fig. S5A), and the phylogenetic analyses indicated that RsHV2 and Cryphonectria hypovirus 4 proteases cluster together (Supplementary Fig. S5B). The RdRp contains six typical motifs, and the catalytic motif 'GDD' was substituted with the alternative 'SDD', as detected in hypoviruses, such as Cryphonectria hypovirus 1 (Supplementary Fig. S6A). The RdRp domain alignment showed that the RsHV2 shares identities ranging from eleven to eighteen per cent with previously reported hypoviruses (Supplementary Table S2A). The RdRp domain phylogenetic tree was consistent with that of the whole ORF2 polyprotein (Supplementary Fig. S6B). Hel2 is located at the C terminus of the ORF2 polyprotein (Fig. 1D) and has six conserved motifs (Supplementary Fig. S4A), the typical hallmark of SFII helicases (Koonin et al. 1993). Hel2 showed 59.75 per cent and 32.35 per cent identities with the RsHV1 and SsHV2 helicases, respectively. Phylogenetic analysis of the helicase region revealed that RsHV2 forms an independent branch with RsHV1 (group IV), which is close to two other hypovirus groups (III and VII) (Supplementary Fig. S4B). In summary, all phylogenetic trees constructed based on the ORF2-encoded proteins indicated that RsHV2 and RsHV1 are closely related, and distinct from all other hypoviruses, justifying the creation of a separate genus, Rhizochypovirus, within the *Hypoviridae* family.

3.4 The RsHV2 ORF1-encoded helicase is related to nidoviruses and also forms an evolutionary link between (+)ssRNA viruses and bacteria

Hel1 contains six conserved motifs typical of SFI helicase hallmarks in (+)ssRNA viruses (Supplementary Fig. S7). BLASTp analysis revealed that it is most closely related to the hypothetical protein encoded by Rhizoctonia solani putative virus 2 (RsPV2; accession number: QDW81315, 43.91% identity, 65% coverage). PSI-BLAST analysis restricted to viruses (taxid: 10239) revealed that Hel1 shares similarity to virgavirus and coronavirus helicases, and this latter observation was supported by

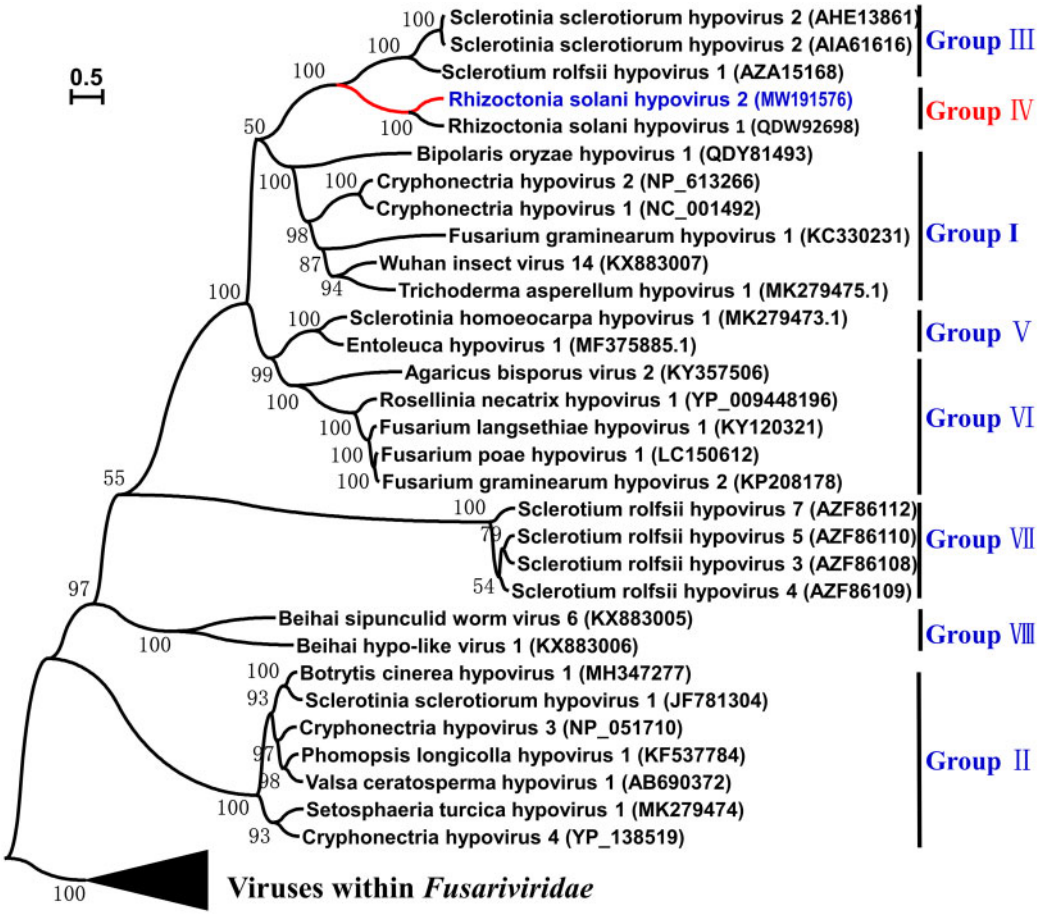

Figure 2. ML phylogenetic tree constructed based on the polyprotein of RsHV2 (highlighted in blue color) and related sequences. All selected hypoviruses were divided into eight groups, and RsHV2 belongs to group IV marked by red color. Numbers on branches indicate bootstrap support. The virus name follows the accession number in parentheses. The members of the proposed family Fusariviridae were used as an out-group. The genetic distance was shown by the upper left scale bar.

multiple sequence alignment results (Supplementary Fig. S7A). RsHV2 and RsPV2 helicases were clustered together into a large group with bacteria and *Nidovirales* members. Conversely, *Virgaviridae* members were grouped with *Benyviridae* members, suggesting that RsHV2 Hel1 is more closely related to *Nidovirales* than other viruses with SFI helicase. Nevertheless, RsHV2 and RsPV2 are closer to endornaviruses than members of *Virgaviridae* and *Benyviridae* (Fig. 3).

We next compared the complex 3D structure of RsHV2 Hel1 with all structures in the Protein Data Bank (PDB). The top four hits were Tomato mosaic virus (ToMV) helicase (PDB code: c3vkwA; 98.7% confidence; 21% identity), arterivirus nonstructural protein 10 helicase (PDB code: c4n0oC; 98.6% confidence; 20% identity), Middle East respiratory syndrome (MERS) coronavirus 2 helicase (PDB code: c5wwpA; 97.8% confidence; 20% identity), and the human upf1 helicase (PDB code: c2gk7A; 97.8% confidence; 19% identity) (Fig. 4). Thus, Hel1 has a structure similar to that of helicases from coronaviruses and ToMV. The results of both the phylogenetic analysis and the 3D structure comparison indicated that the helicases of coronaviruses and RsHV2 originated from a common ancestor compared to those of other viruses. Beyond the evolutionary relationships with other viruses, the Hel1 shared the highest similarity with helicase-related proteins derived from bacteria (approximately 30% identity) (Supplementary Fig. S7B). The maximum likelihood (ML) phylogenetic tree showed that RsHV2 and RsPV2 form a distinct subgroup outside of the virus-related clade with some similarities to bacteria (Fig. 3). Moreover, both RsHV2 and RsPV2 are closer to the root position than bacteria. These results suggested that RsHV2 and RsPV2 helicases might represent intermediates in the evolution of helicases between (+)ssRNA viruses and bacteria via HGT events.

3.5 RsHV2 is associated with hypovirulence

To investigate the effects of RsHV2 on *R. solani* strain XN84, protoplast regeneration was conducted to eliminate the virus. Twenty single-protoplast isolates were selected and regenerated. Eighteen isolates showed colony morphology similar to that of the parental virulent strain XN84, whereas two were morphologically distinct. All isolates were screened for the presence of RsHV2 using RT-PCR amplification with specific primers (RsHV2-F11/R11). Two isolates, one of them designated XN84VF, were successfully cured as confirmed by RT-PCR amplification (Supplementary Fig. S1A) and northern blotting (Fig. 1C). The cured isolates displayed distinct colony morphology as compared to the parental strain (Fig. 1A). Moreover, XN84VF displayed no alteration in growth rate on PDA but did produce more sclerotia than XN84. Strain XN84 differed marginally from XN84VF biologically in producing fewer and smaller lesions on detached rice leaves 3 dpi (Fig. 1B), suggesting hypovirulence. Moreover, RsHV2 could be transferred horizontally to *R. solani* strain ES63 with which is normally vegetatively incompatible with strain XN84 (Supplementary Fig. S2C). Successful transmission was

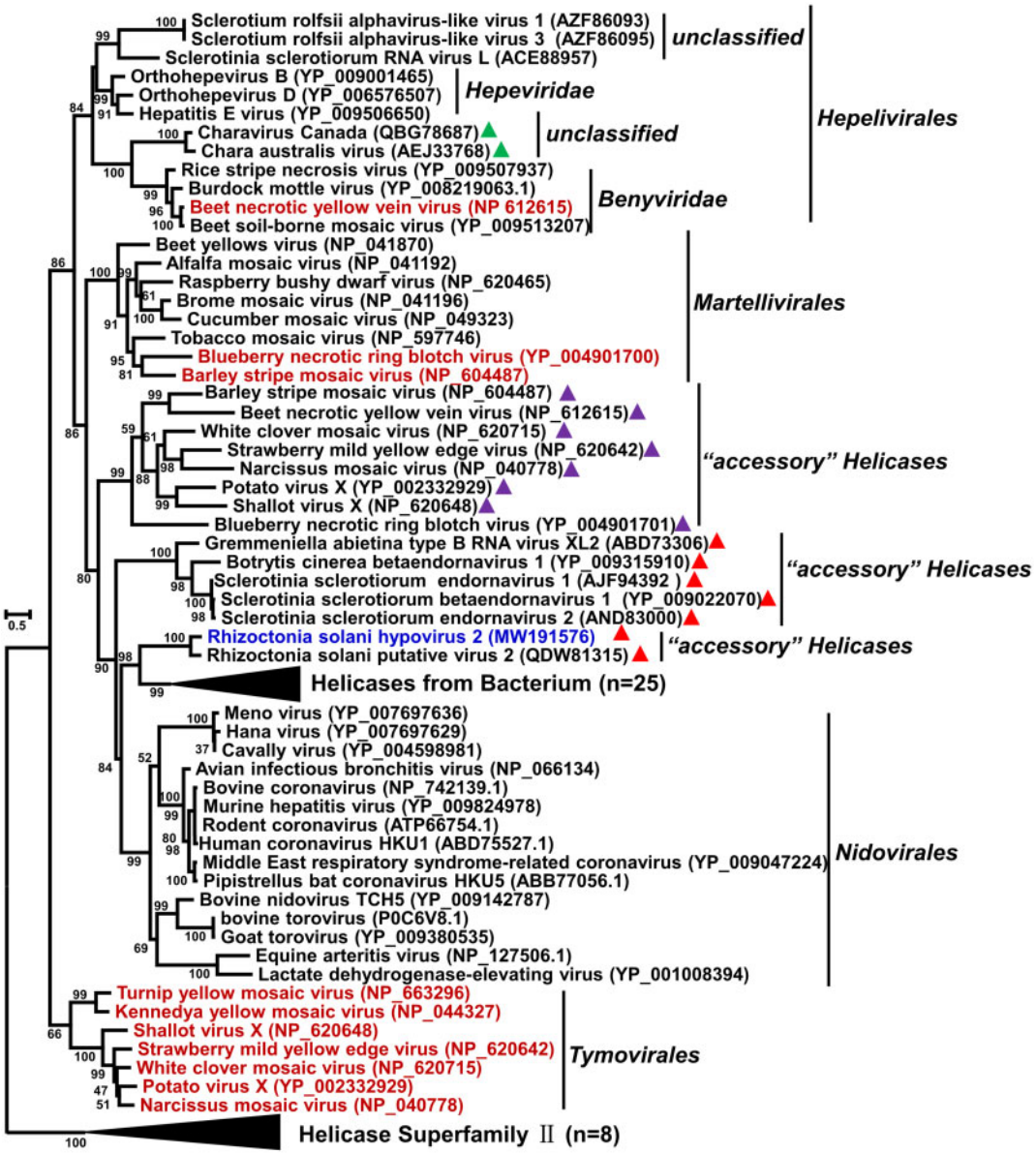

Figure 3. ML phylogenetic tree constructed based on the helicases encoded by RsHV2 (highlighted in blue color) ORF1 and its related viruses. The viruses (Highlighted in red color) have two helicase domains belonging to superfamily I in their genomes, and their "accessory" helicases (▲) were acquired via gene duplication event in the putative common ancestor. Two helicases of RsHV2, RsHV1, and some endornaviruses belong to two different superfamilies, and their 'accessory' helicase group (▲) were obtained from members belonging to superfamily I by the HGT mechanism. Two viruses (▲) including Charavirus and Chara australis virus contain two helicases, but their 'accessory' helicases belong to superfamily II. Numbers on the branches indicate bootstrap support, and the branch lengths were drawn to scale. The genetic distance was shown by the lower left scale bar. The virus name follows the accession number in parentheses. Helicases belonging to superfamily were used as an out-group.

confirmed by RT-PCR amplification (Supplementary Fig. S2B) and dsRNA isolation followed by S1 nuclease, and DNase I treatment (Supplementary Fig. S2A). To determine the complete virome of *R. solani* strain XN84 high-throughput sequencing was conducted twice and the results obtained illustrate that the fungus harbored two mitoviruses and RsHV2, later confirmed by RT-PCR amplification (Supplementary Fig. S1A, Table S1).

4. Discussion

Although mycovirus characterization still lags behind that of viruses infecting other living organisms, mycoviruses are an essential part of the virosphere since they are widespread in the fungal kingdom, and some have unique characteristics. Hence, discovering novel mycoviruses can provide invaluable information regarding the evolution of the virosphere and supply clues for tracing viruses or their components. We identified and characterized a novel mycovirus, RsHV2, related to members of the family *Hypoviridae*. RsHV2 Hel1 is related to the order *Nidovirales*, including coronavirus helicases. Analysis of the RsHV2 genome revealed that multiple potential HGT and recombination events might have occurred during long-term evolution, which could supply new insights into the traceability and evolution of viruses.

The RsHV2 ORF2-encoded polyprotein shares the typical hallmark domains of hypoviruses in the family *Hypoviridae*,

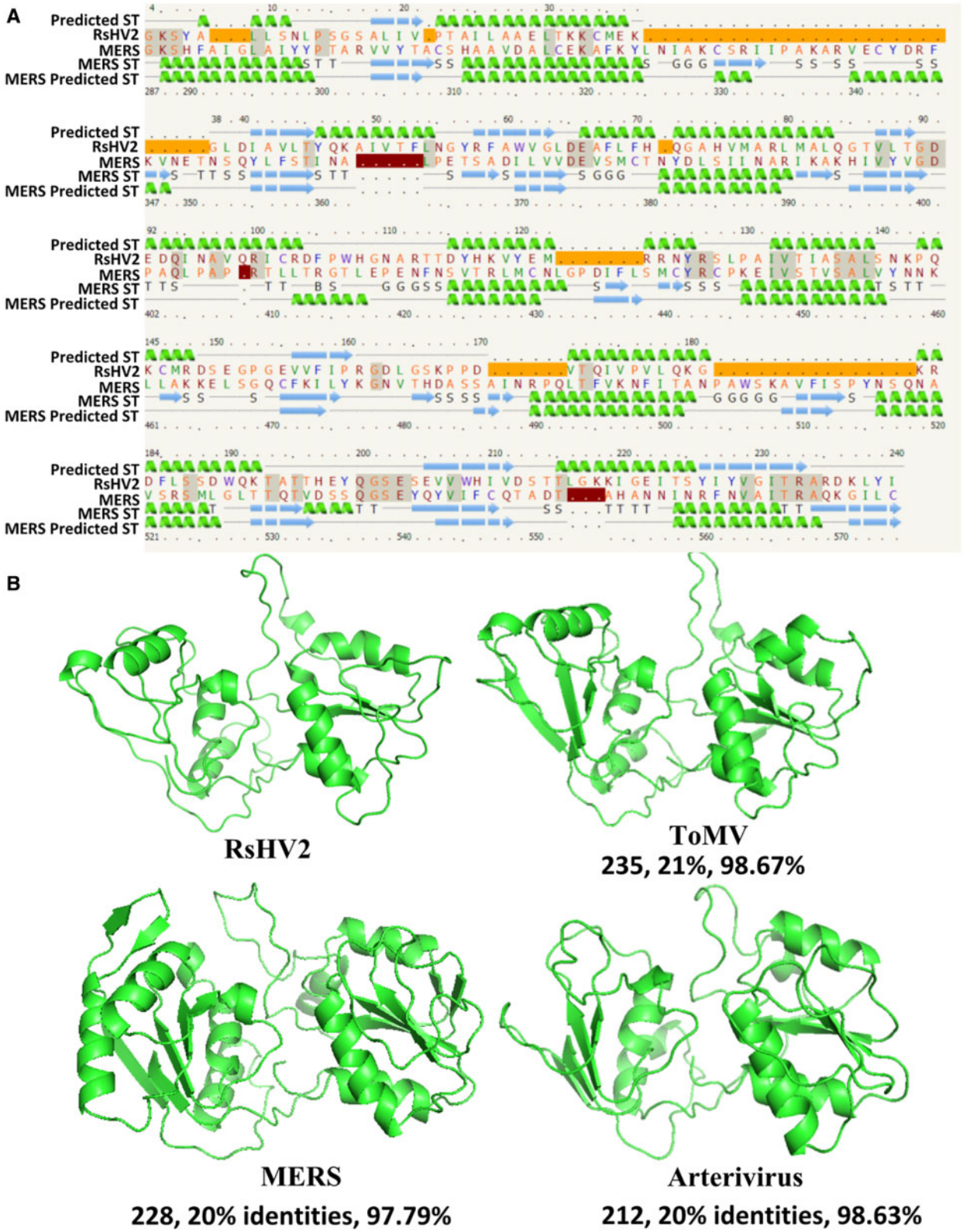

Figure 4. Alignment and 3D structures. (A) Sequence alignment of the ORF1-encoded helicase domain from RsHV2 and MERS (Middle East Respiratory Syndrome) coronavirus 2 (PDB code c5wwpA). Identical residues are highlighted in grey. Green helices represent α-helices, blue arrows indicate β-strands, and light gray lines indicate coil. G, T, B, and S in the 'MERS ST' section represent 3-turn helix (310 helices), hydrogen-bonded turn, residue in isolated β-bridge, and bend, respectively. Orange rectangles represent missing RsHV2 aa residues that are present in the MERS coronavirus 2 sequence. Residues are colored according to a simple property-based scheme, and the position in the original sequence is indicated in the top or bottom line. Predicted ST, Predicted Secondary Structure; MERS ST, MERS Secondary Structure; MERS Predicted ST, MERS Predicted Secondary Structure. (B) The 3D models comparison of RsHV2 ORF1-encoded helicase domain and helicases from MERS coronavirus 2 helicase (PDB code: c5wwpA; 97.8% confidence; 20% identity), arterivirus nonstructural protein 10 helicase (PDB code: c4n0oC; 98.6% confidence; 20% identity), and ToMV (PDB code: c3rnvA; 98.67% confidence; 21% identity). Phyre2 generated the 3D structural models.

suggesting that RsHV2 should be considered a novel member of *Hypoviridae*. However, the molecular features of the RsHV2 genome are significantly distinct from those of all currently reported hypoviruses. First, all reported *Hypoviridae* members contain a (+)ssRNA genome <18 kb in size (Picarelli et al. 2019). However, the RsHV2 genome is 22.2 kb in length, representing the largest hypovirus genome reported to date and, to our knowledge, the largest mycovirus genome reported to date. Secondly, two hypoviruses, Fusarium graminearum hypovirus 1 (FgHV1) (Wang et al. 2013) and Rosellinia necatrix hypovirus 2 (RnHV2) (Arjona-Lopez et al. 2018), have two discontinuous ORFs separated by an intergenic region of approximately 300 nt. The RsHV2 ORFs were separated by a large intergenic region (822 nt), noticeably longer than that in all reported hypoviruses to date. Thirdly, all known hypoviruses contain a single helicase domain in their polyprotein, while two helicase domains are found in RsHV2, one in each helicase. In addition, the RsHV2 ORF1-encoded protein is similar to one recently reported in RsPV2 (43.91% identity) and the ORF2-encoded protein of MoHVA (29% identity), whereas the ORF2-encoded protein shares 49.52 per cent and 38 per cent identity with the equivalent proteins of RsHV1 and MoHVA (Supplementary Fig. S1C). RsPV2 and RsHV1 were recently reported in the *R. solani* population and were considered two unrelated viruses (Picarelli et al. 2019). Notably, RsPV2 does not encode an RdRp which is essential for replication (Picarelli et al. 2019). The possibility exists that RsHV1 and RsPV2 coinfected a single strain of *R. solani*, and that a recombination event between the two occurred facilitating replication of RsPV2. Thus, RsHV2 may be a hybrid virus derived from the recombination of two mycoviruses related to RsPV2 and RsHV1 in the same host, *R. solani*. Additionally, MoHVA ORF3 encodes a single hypovirus-like helicase, whereas MoHVA ORFs (1 and 2) encode proteins with unknown function and lack a second helicase similar to the RsHV2 ORF1-encoded protein (Supplementary Fig. S1C).

Helicases are hallmark genes for nearly all (+)ssRNA viruses with genome sizes over 6 kb and play pivotal roles in a diverse range of biological functions during viral genome replication. Usually, viruses encode a single helicase located close to other replication-associated proteins. Nevertheless, certain viral RNA genomes encoded two helicases of the same family in most cases and rarely of a different family. Viruses accommodating two helicases include endornaviruses (Tuomivirta et al. 2009), tymo-like viruses (Koonin et al. 1993), blunerviruses (Quito-Avila et al. 2013), and several unclassified viruses (Gibbs et al. 2011). These helicases are either located on the same viral segment (Sclerotinia sclerotiorum betaendornavirus 1; Accession number: YP_008169851.1), or different viral segments (Blueberry necrotic ring blotch virus; Accession number: YP_004901700.1 and YP_004901701.1). RsHV2 contains a single segment with two ORFs each encoding a putative helicase domain, SFI and SFII, respectively. Some endornaviruses also encode two helicases, SFI and SFII, on a single polyprotein (Tuomivirta et al. 2009), while Chara australis virus (CAV; Accession number: JF824737.1, unclassified virus) encodes two helicases SFI and SFII similar to RsHV2. The RsHV2 helicases are phylogenetically distant from the CAV helicases. In other examples, tymo-like viruses encode two putative SFI helicases where the first is involved in replication while the second (or accessory) helicase has evolved additional biological functions, is implicated in virus silencing and/or inter-cell movement in plants and is thought to have evolved by gene duplication (Koonin et al. 1993; Morozov and Solovyev 2015). However, while the RsHV2 helicases are phylogenetically distant from the tymo-like virus helicases it would be of interest to investigate whether the RsHV2 helicase(s) confer additional biological functions too. In all aforementioned cases, it is likely that the "accessory" helicases were acquired *via* HGT events.

The phylogenetic relationship between mycoviruses and other viruses is still mostly unexplored. Coronaviruses and related viruses within the order *Nidovirales* are frequently associated with respiratory and enteric diseases in humans, livestock, and domestic animals (Corman et al. 2018; Hasoksuz et al. 2002). Our current work revealed that RsHV2 Hel1 shares aa identity and structural similarity with animal viruses from the family *Nodaviridae* but not other mycoviruses including hypoviruses. Based on our phylogenetic analysis, nidovirus helicases form a branch together with RsHV2 and RsPV2; but nidoviruses were closer to the root than RsHV2 and RsPV2. Therefore, RsHV2 Hel1 and nidovirus helicases share a common ancestry. RsHV2 and its relatives likely acquired the 'accessory' helicase from nidoviruses *via* HGT. Previous studies of mycoviruses revealed close relationships with plant viruses (Donaire et al. 2016), which might be explained by fungal/plant associations through a parasitic or symbiotic relationship over an extended evolutionary time period (Tisserant et al. 2013) where viruses could interact with both fungi and plants. For instance, the hypovirus replicative module (helicase and RdRp) originated from an ancestor belonging to *Potyviridae* (Dawe and Nuss 2013; Dolja and Koonin 2018). The evolutionary origins of mycoviruses are not limited to plant viruses. A recent viral metagenomic investigation generated massive amounts of data and revealed that numerous viruses from invertebrates are phylogenetically related to mycoviruses (Shi et al. 2018; Wu et al. 2020), but evidence of any relationships of mycoviruses with animal viruses is scarce. The presence of an "accessory" helicase in the genome of RsHV2 might represent novel evidence for horizontal transfer between a mycovirus and nidoviruses, but much work is still needed to confirm this.

Like humans, bacteria face a daily threat of infection by viruses. Viruses have shaped the phylogenetic diversity of bacterial communities (Rodriguez-Valera et al. 2009). However, the potential evolutionary links between viral and bacterial pathogens remain a bottleneck, mainly due to the lack of knowledge regarding their full host range (Džunková et al. 2019). In addition to nidoviruses, Hel1 SFI also displayed a high aa identity with bacterial helicases in a homology search. Interestingly, the phylogenetic inference of predicted SFI helicase domains indicates a virus–host linkage. The bacteria form a well-supported cluster and most likely acquired this helicase via HGT, indicating a long-term association between viruses and bacteria. Phylogenetic analysis suggested that the RsHV2 Hel1 shares a common ancestor with other viruses and bacteria. Collectively, these data suggested that HGT had occurred between viruses and bacteria. Notably, previous studies showed a close similarity between cellular proteins and viral helicases (Gorbalenya and Koonin 1993). It will be of invaluable interest to determine whether RsHV2 could horizontally or vertically infect bacteria, suggesting a broad host range, and to determine the role RsHV2 might play in fungal–bacterial interactions.

In summary, RsHV2 is a complex mycovirus containing two putative helicases (SFI and SFII) with relatively distant domains. Hel1 is very similar to nidovirus helicases and cellular proteins, such as coronaviruses and bacteria, respectively, whereas Hel2 showed similarity to typical hypoviruses. RsHV2 presence offers evidence of recombination between viruses and bacteria as well as between fungal viruses and animal viruses. Whether RsHV2 plays a crucial role in fungal–bacterial interactions remains to

be determined, as does the direction of gene (helicase) transfer between bacteria and viruses.

Supplementary data

Supplementary data are available at *Virus Evolution* online.

Acknowledgments

We would like to thank Dr. Huiquan Liu in Northwest A&F University for constructive suggestions on the phylogenetic analysis and Dr. Robert H.A. Coutts in University of Hertfordshire for the critical reading of the manuscript.

Author contributions

J.X., D.J., and A.H.A. designed research; A.H.A., D.H., and Q.T. performed research; J.X., D.J., A.H.A., D.H., Q.T., Y.F., J.C., Y.L., B.L., and I.K.-L. analyzed data; and J.X., D.J., A.H.A., and I.K.-L. wrote the paper.

Funding

This work was financially supported by the National Key Research and Development Program of China (2017YFD0201100), the Natural Science Foundation of China (31722046), and the Fundamental Research Funds for the Central Universities (2662018PY041).

Conflict of interest

The authors herein declare no potential competition of interest.

Data availability

The RsHV2 genome sequence has been deposited in the GenBank database: Accession no. MW191576 in NCBI (https://www.ncbi.nlm.nih.gov/).

References

Aaziz, R., and Tepfer, M. (1999) 'Recombination in RNA Viruses and in Virus-Resistant Transgenic Plants', *Journal of General Virology*, 80: 1339–46.

Alexander, W. G. et al. (2016). 'Horizontally Acquired Genes in Early-Diverging Pathogenic Fungi Enable the Use of Host Nucleosides and Nucleotides'. *Proceedings of the National Academy of Sciences*, 113: 4116–21.

Andersson, J. O. (2009) 'Gene Transfer and Diversification of Microbial Eukaryotes', *Annual Review of Microbiology*, 63: 177–93.

Arjona-Lopez, J. M. et al. (2018) 'Novel, Diverse RNA Viruses from Mediterranean Isolates of the Phytopathogenic Fungus, *Rosellinia Necatrix*: Insights into Evolutionary Biology of Fungal Viruses', *Environmental Microbiology*, 20: 1464–83.

Baltimore, D. (1971) 'Expression of Animal Virus Genomes', *Bacteriological Reviews*, 35: 235–41.

Bejarano, E. R. et al. (1996) 'Integration of Multiple Repeats of Geminiviral DNA into the Nuclear Genome of Tobacco During Evolution'. *Proceedings of the National Academy of Sciences*, 93: 759–64.

Bentley, K., and Evans, D. J. (2018) 'Mechanisms and Consequences of Positive-Strand RNA Virus Recombination', *Journal of General Virology*, 99: 1345–56.

Bräutigam, A. et al. (2011) 'Critical Assessment of Assembly Strategies for Non-Model Species mRNA-Seq Data and Application of Next-Generation Sequencing to the Comparison of C3 and C4 Species', *Journal of Experimental Botany*, 62: 3093–102.

Corman, V. M. et al. (2018) 'Hosts and Sources of Endemic Human Coronaviruses', *Advances in Virus Research*, 100: 163–88.

Crickard, J. B. et al. (2020) 'Rad54 Drives ATP Hydrolysis-Dependent DNA Sequence Alignment during Homologous Recombination', *Cell*, 181: 1380–94.

Dawe, A. L., and Nuss, D. L. (2013) 'Hypovirus Molecular Biology: From Koch's Postulates to Host Self-Recognition Genes That Restrict Virus Transmission', *Advances in Virus Research*, 86: 109–47.

Dolja, V. V., and Koonin, E. V. (2018) 'Metagenomics Reshapes the Concepts of RNA Virus Evolution by Revealing Extensive Horizontal Virus Transfer', *Virus Research*, 244: 36–52.

Donaire, L. et al. (2016) 'Characterization of *Botrytis Cinerea* Negative-Stranded RNA Virus 1, a New Mycovirus Related to Plant Viruses, and a Reconstruction of Host Pattern Evolution in Negative-Sense ssRNA Viruses', *Virology*, 499: 212–8.

Kearse, M. et al. (2012) 'Geneious Basic: An Integrated and Extendable Desktop Software Platform for the Organization and Analysis of Sequence Data', *Bioinformatics (Oxford, England)*, 28: 1647–9.

Džunková, M. et al. (2019) 'Defining the Human Gut Host-Phage Network through Single-Cell Viral Tagging', *Nature Microbiology*, 4: 2192–203.

Feng, H. et al. (2012) 'Preparation, Purification and Regeneration Optimizing Research of Protoplasts from *Rhizoctonia solani*', *African Journal of Microbiology Research*, 6: 3222–30.

Fiers, M. et al. (2011) 'Genetic Diversity of *Rhizoctonia solani* Associated with Potato Tubers in France', *Mycologia*, 103: 1230–44.

Garg, R. et al. (2011) 'De Novo Assembly of Chickpea Transcriptome Using Short Reads for Gene Discovery and Marker Identification', *DNA Research: An International Journal for Rapid Publication of Reports on Genes and Genomes*, 18: 53–63.

Ghabrial, S. A. et al. (2015) '50-plus Years of Fungal Viruses', *Virology*, 479: 356–68.

Gibbs, A. J. et al. (2011) 'The Enigmatic Genome of Chara Australis Virus', *Journal of General Virology*, 92: 2679–90.

Gogarten, J. P., and Townsend, J. P. (2005) 'Horizontal Gene Transfer, Genome Innovation and Evolution', *Nature Reviews. Microbiology*, 3: 679–87.

Gorbalenya, A. E., and Koonin, E. V. (1993) 'Helicases: Amino Acid Sequence Comparisons and Structure-Function Relationships', *Current Opinion in Structural Biology*, 3: 419–29.

Hasoksuz, M. et al. (2002) 'Detection of Respiratory and Enteric Shedding of Bovine Coronaviruses in Cattle in an Ohio Feedlot', *Journal of Veterinary Diagnostic Investigation*, 14: 308–13.

Jiang, D., and Ghabrial, S. A. (2004) 'Molecular Characterization of Penicillium chrysogenum Virus: Reconsideration of the Taxonomy of the Genus Chrysovirus', *Journal of General Virology*, 85: 2111–21.

Katzourakis, A. et al. (2007) 'Discovery and Analysis of the First Endogenous Lentivirus'. *Proceedings of the National Academy of Sciences*, 104: 6261–65.

Keeling, P. J., and Palmer, J. D. (2008) 'Horizontal Gene Transfer in Eukaryotic Evolution', *Nature Reviews. Genetics*, 9: 605–18.

Kelley, L. A. et al. (2015) 'The Phyre2 Web Portal for Protein Modeling, Prediction, and Analysis', *Nature Protocols*, 10: 845–58.

Khalifa, M. E., and Pearson, M. N. (2014) 'Characterisation of a Novel Hypovirus from *Sclerotinia sclerotiorum* Potentially Representing a New Genus within the Hypoviridae', *Virology*, 464: 441–9.

Koonin, E. V. et al. (1993) 'Evolution and Taxonomy of Positive-Strand RNA Viruses: Implications of Comparative Analysis of Amino Acid Sequences', *Critical Reviews in Biochemistry and Molecular Biology*, 28: 375–30.

Kotta-Loizou, I., and Coutts, R. H. A. (2017) 'Mycoviruses in *Aspergilli*: A Comprehensive Review', *Frontiers in Microbiology*, 8: 1699.

Krogh, A. et al. (2001) 'Predicting Transmembrane Protein Topology with a Hidden Markov Model: Application to Complete Genomes', *Journal of Molecular Biology*, 305: 567–80.

Kumar, S. et al. (2018) 'MEGA X: Molecular Evolutionary Genetics Analysis across Computing Platforms', *Molecular Biology and Evolution*, 35: 1547–9.

Lai, M. M. (1992) 'RNA Recombination in Animal and Plant Viruses', *Microbiology and Molecular Biology Reviews*, 56: 61–79.

Lamberto, I. et al. (2014) 'Mycovirus-like DNA Virus Sequences from Cattle Serum and Human Brain and Serum Samples from Multiple Sclerosis Patients', *Genome Announcements*, 2: 848–14.

Li, P. et al. (2015) 'Molecular Characterization of a Novel Hypovirus from the Plant Pathogenic Fungus *Fusarium graminearum*', *Virology*, 481: 151–60.

Li, Q. et al. (2020) 'The Complete Genome Sequence of a Novel Hypovirus Infecting *Bipolaris Oryzae*', *Archives of Virology*, 165: 1027–5.

Liu, H. et al. (2010) 'Widespread Horizontal Gene Transfer from Double-Stranded RNA Viruses to Eukaryotic Nuclear Genomes', *Journal of Virology*, 84: 11876–87.

—— et al. (2011) 'Widespread Horizontal Gene Transfer from Circular Single-Stranded DNA Viruses to Eukaryotic Genomes', *BMC Evolutionary Biology*, 11: 1–15.

Loeffelholz, M. J., and Fenwick, B. W. (2021) 'Taxonomic Changes for Human and Animal Viruses', *Journal of Clinical Microbiology*, 59: 1932–20.

Marcet-Houben, M., and Gabaldón, T. (2010) 'Acquisition of Prokaryotic Genes by Fungal Genomes', *Trends in Genetics: Tig*, 26: 5–8.

Morozov, S. Y., and Solovyev, A. G. (2015) 'Phylogenetic Relationship of Some "Accessory" Helicases of Plant Positive-Stranded RNA Viruses: Toward Understanding the Evolution of Triple Gene Block', *Frontiers in Microbiology*, 6:

Nagy, P. D., and Simon, A. E. (1997) 'New Insights into the Mechanisms of RNA Recombination', *Virology*, 235: 1–9.

Nerva, L. et al. (2016) 'Multiple Approaches for the Detection and Characterization of Viral and Plasmid Symbionts from a Collection of Marine Fungi', *Virus Research*, 219: 22–38.

Parrella, G. et al. (2013) 'First Report of Tomato Spotted Wilt Virus in *Iberis Semperflorens*', *Journal of Plant Pathology*, 95: 69–74.

Picarelli, M. et al. (2019) 'Extreme Diversity of Mycoviruses Present in Isolates of *Rhizoctonia solani* AG2-2 LP from Zoysia Japonica from Brazil', *Frontiers in Cellular and Infection Microbiology*, 9: 244.

Potgieter, A. C. et al. (2009) 'Improved Strategies for Sequence-Independent Amplification and Sequencing of Viral Double-Stranded RNA Genomes', *Journal of General Virology*, 90: 1423–32.

Quito-Avila, D. F. et al. (2013) 'Genetic Characterization of Blueberry Necrotic Ring Blotch Virus, a Novel RNA Virus with Unique Genetic Features', *Journal of General Virology*, 94: 1426–34.

Richards, T. A. et al. (2011) 'Gene Transfer into the Fungi', *Fungal Biology Reviews*, 25: 98–10.

Robinson, J. T. et al. (2017) 'Variant Review with the Integrative Genomics Viewer', *Cancer Research*, 77: e31–34.

Rodriguez-Valera, F. et al. (2009) 'Explaining Microbial Population Genomics through Phage Predation', *Nature Reviews. Microbiology*, 7: 828–36.

Roossinck, M. J. (2019) 'Evolutionary and Ecological Links between Plant and Fungal Viruses', *New Phytologist*, 221: 86–92.

Sahin, E., and Akata, I. (2018) 'Viruses Infecting Macrofungi', *Virusdisease*, 29: 1–18.

Shi, M. et al. (2018) 'The Evolutionary History of Vertebrate RNA Viruses', *Nature*, 556: 197–202.

Son, M., Yu, J., and Kim, K.-H. (2015) 'Five Questions about Mycoviruses', *PLoS Pathogens*, 11: e1005172.

Su, C. L. et al. (2011) 'De Novo Assembly of Expressed Transcripts and Global Analysis of the *Phalaenopsis Aphrodite* Transcriptome', *Plant & Cell Physiology*, 52: 1501–14.

Su, S. et al. (2016) 'Epidemiology, Genetic Recombination, and Pathogenesis of Coronaviruses', *Trends in Microbiology*, 24: 490–02.

Suzuki, N., ICTV Report Consortium. et al. (2018) 'ICTV Virus Taxonomy Profile: *Hypoviridae*', *Journal of General Virology*, 99: 615–6.

Svoboda, P., and Cara, A. D. (2006) 'Hairpin RNA: A Secondary Structure of Primary Importance', *Cellular and Molecular Life Sciences: CMLS*, 63: 901–8.

Thomas, C. M., and Nielsen, K. M. (2005) 'Mechanisms of, and Barriers to, Horizontal Gene Transfer between Bacteria', *Nature Reviews. Microbiology*, 3: 711–21.

Tisserant, E. et al. (2013) 'Genome of an Arbuscular Mycorrhizal Fungus Provides Insight into the Oldest Plant Symbiosis'. *Proceedings of the National Academy of Sciences*, 110: 20117–22.

Tuomivirta, T. T. et al. (2009) 'A Novel Putative Virus of *Gremmeniella Abietina* Type B (*Ascomycota*: *Helotiaceae*) Has a Composite Genome with Endornavirus Affinities', *Journal of General Virology*, 90: 2299–05.

Wang, S. et al. (2013) 'A Novel Virus in the Family *Hypoviridae* from the Plant Pathogenic Fungus *Fusarium graminearum*', *Virus Research*, 174: 69–77.

Wang, Z. et al. (2009) 'RNA-Seq: A Revolutionary Tool for Transcriptomics', *Nature Reviews. Genetics*, 10: 57–63.

Wisecaver, J. H., and Rokas, A. (2015) 'Fungal Metabolic Gene Clusters-Caravans Traveling across Genomes and Environments', *Frontiers in Microbiology*, 6.

—— et al. (2014) 'The Evolution of Fungal Metabolic Pathways', *PLoS Genetics*, 10: e1004816.

Wu, H. et al. (2020) 'Abundant and Diverse RNA Viruses in Insects Revealed by RNA-Seq Analysis: Ecological and Evolutionary Implications', *mSystems*, 5: 39–20.

Xia, Y. et al. (2017) 'Transcriptome Analysis Reveals the Host Selection Fitness Mechanisms of the *Rhizoctonia solani* AG1IA Pathogen', *Scientific Reports*, 7: 1–16.

Xie, J. et al. (2006) 'Characterization of Debilitation-Associated Mycovirus Infecting the Plant-Pathogenic Fungus *Sclerotinia sclerotiorum*', *Journal of General Virology*, 87: 241–9.

Yuan, W., and Hillman, B. I. (2001) 'In Vitro Translational Analysis of Genomic, Defective, and Satellite RNAs of Cryphonectria Hypovirus 3-GH2', *Virology*, 281: 117–23.

Zhang, L. et al. (2009) 'A Novel Virus That Infecting Hypovirulent Strain XG36-1 of Plant Fungal Pathogen *Sclerotinia sclerotiorum*', *Virology Journal*, 6: 96– 9.

Zuker, M. (2003) 'Mfold Web Server for Nucleic Acid Folding and Hybridization Prediction', *Nucleic Acids Research*, 31: 3406–15.